Modeling Part Dynamics and Chatter Stability In Machining Considering Material Removal

S. Atlar[1], E. Budak[2], H. N. Özgüven[1]
[1] Middle East Technical University, Ankara, Turkey
[2] Sabanci University, Istanbul, Turkey
[2] Corresponding author: ebudak@sabanciuniv.edu

Abstract
The frequency response function (FRF) of the structures involved in the cutting system must be known for the generation of the stability diagrams. When the flexibility of the workpiece is significant, besides the FRF of the spindle-tool holder-tool assembly, the dynamics of the workpiece must also be included in the overall FRF of the system. In this paper, an exact structural modification method is used to find the FRFs of the workpiece at every stage of the machining process. The system matrices and the modal parameters of the original structure are extracted from a commercial finite element program. Then, the stability diagram of the system is obtained at different stages of machining. The effects of varying dynamics of the workpiece, different cutting conditions and machining strategies on the stable material removal rates and total machining times are studied extensively through case studies.

Keywords
Chatter Stability, Part Dynamics, Structural Modification.

1 INTRODUCTION

Self-excited vibration which is called "*chatter*" is one of the most common problems in machining. Chatter vibrations develop due to dynamic interactions between the cutting tool and workpiece, and result in poor surface finish and reduced tool life and productivity. Regenerative type chatter occurs due to variation in the chip thickness during the machining processes. Stability lobe diagrams can be used to determine chatter-free machining conditions and to maximize stable material removal rate. These diagrams are based on the frequency response functions (FRFs) of the system. Since chatter is a result of the relative movement between the cutting tool and the workpiece, the dynamics of the workpiece (especially for thin-walled and slender structures) play a very important role on the generation of stability lobe diagrams. Furthermore, during a cutting process, the dynamics of the workpiece changes continuously due to material removal. As a result, in order to predict more realistic stability lobe diagrams, the dynamics the workpiece must be updated for every stages of the process.

Taylor [1] stressed the importance of chatter and difficulty in its suppression exactly one century ago (1907). However, until 1950s no analytical method or solution was developed on chatter problems. Tobias et al. [2, 3] and Tlusty and Polacek [4] established the basis of the regenerative chatter theory and generated stability models for orthogonal cutting. A feedback model explaining chatter as a closed loop interaction between the structural dynamics and the cutting process was presented by Merrit [5]. In turning, the orientation of the cutting forces and chip thickness are not a function of time, however in milling the cutting forces, chip thickness and the direction of the excitation vary with time due to rotating cutter. Tlusty and Koenigsberger [6] adapted their orthogonal cutting chatter stability model to milling process considering an average direction and average number of teeth in cut to find stability lobes. Opitz et al. [7, 8] generated an improved lumped model in the average force direction. Tlusty et al. [9-11] presented a method of generating stability lobes using time domain simulations of the chatter vibrations in milling. Sridhar et al. [12, 13] derived a detailed dynamic force formulation in milling. Minis and Yanushevsky [14, 15] used Floquet's Theorem and Fourier series for milling stability formulation. Then, using the Nyquist criterion they solved the problem numerically. Altintas and Budak [16] presented a new method for the analytical prediction of stability limits in milling. Their analytical method was verified with numerical and experimental results and presented for the generation of the stability lobe diagrams [17].

In order to form the stability diagrams, the dynamic response of the machine tool structure is required. Tool point FRFs are usually measured using impact testing and modal analysis [18]. Considering great variety of machine tool configurations, tool holder and cutting tool geometries, to make a new test for every combination can be quite time consuming and impractical. In a recent study, Ertürk et al. [19, 20] presented an analytical approach to predict the tool point FRF by modeling the whole system (spindle, tool holder and tool). They also analyzed the effects of bearing supports, and spindle-holder and tool-holder interfaces on the FRF [21], and demonstrated the use of the model in fast and practical generation of the stability diagrams [22].
If the workpiece to be machined is dynamically flexible, in order to obtain the stability limits correctly the workpiece dynamics must be included in the analysis. However, the dynamics of the workpiece continuously vary during machining due to the mass removal. Thus, the variation of the dynamics of the workpiece must also be considered in the generation of the stability lobes. At this point, it becomes very important to use an efficient structural modification method in order to find the frequency response functions of the modified (machined) structures at intermediate steps of the machining process. Many different reanalysis techniques are available in literature. Özgüven has developed a structural modification method using FRFs of the original structure and system matrices of the modifying structure [23-25]. Özgüven first introduced the matrix inversion method to obtain the receptances of a damped system from its undamped counterparts [23]. Then, he presented a new method to calculate FRFs of non-proportionally damped structures using undamped modal data without matrix inversion [24]. Both of these methods can be applied to the structural modification problems as explained in [25] where the method is also extended to structural modifications with additional degrees of freedom.
In this paper, the effects of part dynamics and its variation on the chatter stability are analyzed through modeling. In addition, the effects of different cutting conditions and machining strategies on the stable material removal rate are also studied in detail by various case studies. An exact structural modification method is used to find the FRFs of the workpiece at every stage of the machining process. In order to obtain the system matrices and the modal parameters of the original structure, a commercial finite element program is used. Then, the stability diagram of the system is obtained by combining the FRF of the tool and the workpiece at different stages of machining. The tool point FRFs are calculated by an analytical modeling approach developed by Ertürk, et al. [19–22], and used in the analytical stability diagram generation [16, 17]. Although the application of the developed method is demonstrated on milling, it can also be extended to turning of flexible parts where the part dynamics may have significant effects on stability limits [26].

2 CHATTER STABILITY

Chatter is the result of the dynamic interactions between the cutting tool and the workpiece. For a certain cutting speed there is a limiting depth of cut above which the system becomes unstable, and chatter develops. The chatter stability limit in orthogonal cutting is given as [6]:

$$b_{\lim} = \frac{-1}{2.K_f.\mathrm{Re}\left[G(\omega)\right]} \tag{1}$$

where K_f is the cutting force coefficient in the feed direction which is measured or calibrated through testing [27], $\mathrm{Re}\left[G(\omega)\right]$ is the real part of the resultant FRF in the chip thickness direction. $G(\omega)$ is the total transfer function of the system which can be determined by summing tool and workpiece transfer functions:

$$\left[G(\omega)\right] = \left[G_{cutter}(\omega)\right] + \left[G_{workpiece}(\omega)\right] \tag{2}$$

The stability analysis of milling is more complicated due to the rotation tool and intermittent cutting action. Budak and Altintas [16, 17] presented an analytical stability model for the generation of stability diagrams. In this model the axial stability limit, a_{lim}, is given as

$$a_{\lim} = -\frac{2.\pi.\Lambda_R}{N.K_t}\left(1+\kappa^2\right) \tag{3}$$

where N is the number of cutting teeth on the tool, Λ_R is the real part of the eigenvalue of the dynamic cutting system, and can be determined from the following expressions [16, 17]:

$$\Lambda = -\frac{1}{2.a_0}\left(a_1 \pm \sqrt{a_1^2 - 4.a_0}\right) \tag{4}$$

where

$$\begin{aligned} a_0 &= G_{xx}(i\omega_c)G_{yy}(i\omega_c)(\alpha_{xx}\alpha_{yy} - \alpha_{xy}\alpha_{yx}) \\ a_1 &= \alpha_{xx}G_{xx}(i\omega_c) + \alpha_{yy}G_{yy}(i\omega_c) \end{aligned} \tag{5}$$

Here G_{xx} and G_{yy} represent the sum of the tool point and workpiece FRFs in x and y directions, respectively, as defined in equation (2). κ is the ratio of the imaginary and the real parts of the eigenvalue:

$$\kappa = \frac{\Lambda_I}{\Lambda_R} = \frac{\sin\omega_c T}{1-\cos\omega_c T} \tag{6}$$

Equation (6) can be solved to obtain a relation between the chatter frequency and the spindle speed [16, 17] as follows:

$$\omega_c T = \varepsilon + 2.k.\pi \quad , \quad \varepsilon = \pi - 2.\psi \quad , \quad \psi = \tan^{-1}\kappa \quad , \quad n = \frac{60}{N.T} \tag{7}$$

where ε is the phase difference between the inner and outer modulations, k is an integer corresponding to the number of vibration waves within a tooth period, and n is the spindle speed (rpm). Therefore, for a given cutting geometry, cutting force coefficients, tool and workpiece FRFs, and a chatter frequency ω_c, Λ_I and Λ_R can be determined from equation (4), and can be used in equations (7) and (3) to determine the corresponding spindle speed and the stability limit. When this procedure is repeated for a range of chatter frequencies and number of vibration waves, *k*, the stability lobe diagram for a milling system is obtained.

3 MODELING OF WORKPIECE DYNAMICS AND ITS EFFECTS ON STABLITY LIMITS

3.1 Matrix Inversion Method

The matrix inversion method presented by Özgüven [23] was originally developed to calculate the FRFs of the damped structures from undamped modal data, and later it was applied to structural modification problems [25]. In this section, the generalized form of the formulation for structural modifications is explained.

Consider a system with n degrees of freedom whose dynamics can be represented as

$$[M]\{\ddot{x}\} + i[H]\{x\} + [K]\{x\} = \{F\} \tag{8}$$

where $[M]$ is the mass matrix, $[H]$ is the structural damping matrix, $[K]$ is the stiffness matrix, $\{\boldsymbol{x}\}$ is the vector of generalized coordinates and $\{F\}$ is a generalized harmonic force vector, for which the response $\{x\}$ can be found as

$$\{x\} = \left[[K] - \omega^2[M] + i[H]\right]^{-1}\{F\} \tag{9}$$

Here ω is the excitation frequency.

Then, the receptance matrix $[\alpha]$ can be written as

$$[\alpha] = \left[[K] - \omega^2[M] + i[H]\right]^{-1} \tag{10}$$

The receptance matrix of the modified system $[\gamma]$ can be written in a similar manner, and then by making some manipulations $[\gamma]$ can be obtained as

$$[\gamma] = [[I] + [\alpha][D]]^{-1}[\alpha] \tag{11}$$

where $[D]$ denotes the dynamic structural modification matrix and is expressed as

$$[D] = [\Delta K] - \omega^2[\Delta M] + i[\Delta H] \tag{12}$$

Here, $[\Delta K]$, $[\Delta M]$ and $[\Delta H]$ are stiffness, mass and damping modification matrices, respectively. When the structural modification is local,

$$[D] = \begin{bmatrix} [D_{11}] & [0] \\ [0] & [0] \end{bmatrix} \tag{13}$$

Then, equation (11) can be written in partitioned form, so that the receptance submatrices of the modified system can be obtained [23] as

$$\begin{aligned} [\gamma_{11}] &= [[I] + [\alpha_{11}][D_{11}]]^{-1}[\alpha_{11}] \\ [\gamma_{12}]^T &= [\gamma_{21}] = [\alpha_{21}][[I] - [D_{11}][\gamma_{11}]] \\ [\gamma_{22}] &= [\alpha_{22}] - [\alpha_{21}][D_{11}][\gamma_{12}] \end{aligned} \tag{14}$$

Subscripts (1) and (2) correspond to the modified and unmodified regions of the structure, respectively. As can be seen from the equations, to find the receptance matrix of a modified system it is sufficient to the take the inverse of a single matrix which has an order equal to the number of coordinates involved in the structural modifications. Therefore, if the modification is made on a small number of coordinates, the computational time will be reduced considerably.

3.2 Variation of Workpiece Dynamics

In order to determine the varying dynamics of the workpiece using the structural modification method, the FRFs of the original structure and the modification matrices (mass, stiffness and damping matrices) are required. For this purpose, first, the workpiece with its final shape and the removed mass are modeled by using the finite element analysis (MSC Marc© was used in this study). Then, the modal parameters and system matrices of the workpiece are obtained through modal analysis. The developed computer code first calculates the receptance of the unmodified structure (final structure) using modal parameters by modal summation formulation:

$$\alpha_{ij}(\omega) = \sum_{r=1}^{N} \frac{\phi_{ir}\phi_{jr}}{\omega_r^2 - \omega^2 + i\gamma\omega_r^2} \tag{15}$$

where $\alpha_{ij}(\omega)$, ϕ, ω_r and γ are the receptance matrix, mass normalized eigenvector, r^{th} eigenfrequency of the system, and the loss factor, respectively. Based on the cutting strategy which defines the workpiece's geometry variation pattern, the workpiece is meshed, and by using an inverse process, the removed material is virtually added to the geometry of the finished workpiece continuously until the original part geometry is obtained. At every machining step, the FRFs of the workpiece is found by the Matrix Inversion Method [23] using the FRF of the main body and the removed section properties. These FRFs are summed with the FRFs of the tool-holder-spindle assembly calculated by an analytical modeling approach [21-24], and used in the analytical stability diagram generation [16, 17].

3.3 Selection of Chatter-Free Conditions for Minimum Machining Time

Since chatter is one of the most important limitations on the productivity and the part quality, prediction of chatter-free conditions becomes very important in order to increase stable mass removal rate and minimize machining time. However, considering a single cycle alone is not sufficient, the whole process must be analyzed as each cycle may affect the others, especially

the part dynamics in subsequent cuts. Therefore, different machining strategies must be considered in order to achieve overall maximum stable material removal rate. In this study, two different approaches are used in order to demonstrate the effects of cutting conditions and part dynamics on machining time.
In the first approach, one common maximum chatter-free depth of cut and spindle speed pair is used for the whole process. In order to determine the chatter-free stable speed and depth of cut for the whole process, the stability diagrams for each cycle are used together to identify the common stable zones. In the second approach, on the other hand, separate stable cutting conditions for each pass of every cycle are used.
Machining time in a milling process is given as,

$$t_m = nop.\frac{l_w}{V_f} \tag{16}$$

where t_m is machining time, nop is number of pass(step), l_w is cutting length in one pass(step) and V_f is feed rate:

$$V_f = N.f_t.n_t \tag{17}$$

where N is the number of teeth (flutes) of the cutter, f_t is feed per tooth (in mm/rev per tooth), n_t is rotational frequency of the cutter (in rpm). Total machining time for different cases are calculated in the following section in order to demonstrate the effects of the machining strategy and the part dynamics on the stable machining time.
The axial depth of cut affects *nop,* and thus the machining time. Therefore, prediction of the maximum stable axial depth of cut becomes very important for increasing productivity. The effect of the radial depth of cut on stability diagrams is also important, and is studied in the next section for different cases. In general, the stable axial depth of cut is inversely proportional to the stable radial depth of cut [28]. Thus, using higher radial depth of cut in machining causes reduction in the stable axial depth of and may result in longer machining times. However, considering existence of many alternative machining strategies and conditions, and nonlinear interdependency between them, it is almost impossible to generalize the results. Thus, these relations are analyzed in representative case studies in the next section. The effect of the different machining strategies on the stability and the machining time is examined, and it is shown that that by using an appropriate cutting pattern selected based on the part geometry, the overall stability limits of the system can be increased and the machining time can be reduced significantly.

4 ANALYSIS OF PART DYNAMICS EFFECTS ON STABILITY AND CHATTER-FREE MACHINING TIME THROUGH CASE STUDIES

In this section, milling cases are analyzed in order to demonstrate the effects of part dynamics on the stable material removal rate. Variation of the part dynamics and its affect on the stability diagrams are demonstrated where tool dynamics is also considered. It is shown that the total FRF at the cutting point vary significantly due to the changes in the part dynamics and the tool-part contact points resulting in drastic changes in stability diagrams. Furthermore, it is also demonstrated that depending on how the resulting stability diagrams are treated in the selection of milling conditions, very different machining times can be obtained demonstrating significant effects of part dynamics on productivity.
In order to obtain FRFs at different stages and locations of the workpiece during machining, as a first attempt, the workpiece is modeled as a beam in a commercial FE program (MSC Marc Mentat©). The workpiece shown in Figure 1 has the length of 100 mm, width of 50 mm with 15 mm thickness. The material is steel with Young's modulus of 200GPa, Poisson's ratio of 0.3 and a density of 7800 kg/m^3. The boundary conditions of the beam are taken as fixed-free. This model resembles a part clamped on the machine tool table such as a turbine or compressor blade, however with simplified geometry. The feed per tooth, f_t, is taken as 0.15 for roughing cycles and 0.1 for semi-finishing and finishing. These values are used for all cases as the effect of the feed on the stability is minimal, but required for machining time calculations. The number

of teeth on the milling cutter, *N*, is 4 and spindle speed is taken as the one corresponding to the maximum axial depth of cut, i.e. the first lobe.

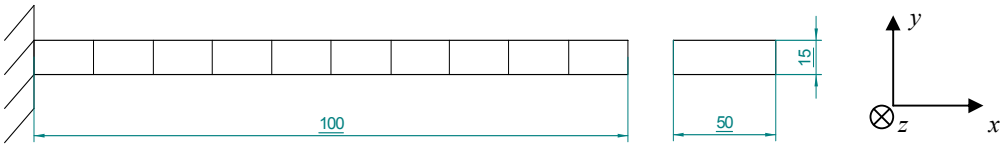

Figure 1: Beam model for the sample part. (Dimensions are in mm).

The workpiece is modeled with beam elements (Element type 5). Each node of the beam element has 3 degrees of freedom (displacement in *x* axis, displacement in *y* axis and rotation around *z* axis) where the total degree of freedom of the model is 30 with 10 elements.
The tool dynamics is also included in the stability analysis using the analytical modeling approach developed by Ertürk, et al. [19-22]. The workpiece is assumed to be machined in three cutting cycles: roughing, semi-finishing and finishing. As an initial assumption, the axial depth of cut is taken as 10 mm so that the workpiece is machined in 10 steps per cut (pass). In order to refer to machining steps a coding convention is used. For example, B15 stands for the 5th step of the 1st cut (roughing cut).

4.1 FRFs of the Workpiece and Stability Diagrams at Different Steps of the Cut

In order to see the variation of the dynamics of the beam clearly, the FRFs of the beam at the same location, but in different cuts are compared to demonstrate the effect of the thickness change of the workpiece on the FRFs and the stability diagrams. By comparing the FRFs of the workpiece at different locations, on the other hand, the effect of the tool movement on the stability limits is observed.
The geometry of the workpiece at the 1st and 9th step of cutting in the roughing, semi-finishing and finishing passes are shown in Figure 2. In order to see the effect of the thickness, the FRFs of the beam B11, B21, B31 and B19, B29, B39 are drawn in Figure 3.
As shown in Figure 3, the magnitude of the FRFs of the workpiece increases as the workpiece becomes thinner as expected. While at the beginning of the process the flexibility of the tool is higher than that of the workpiece, at the end of the process the workpiece dynamics becomes dominant at the end of first step of the cuts. As seen from Figure 3(b), the FRFs of the workpiece near to the fixed end have the lowest values compared to the other locations, as the stiffness of the workpiece is the largest in this region, and thus the FRFs of the workpiece is not effective on the total FRFs of the system. In such a case, only the FRF of the tool can be used to predict the stability diagrams accurately. The natural frequencies of the workpiece reduce while the thickness of the workpiece decreases as shown in Figure 3. The stability lobe diagrams at the end of the first and ninth step of the 1st, 2nd and 3rd cuts are shown in Figure 4.

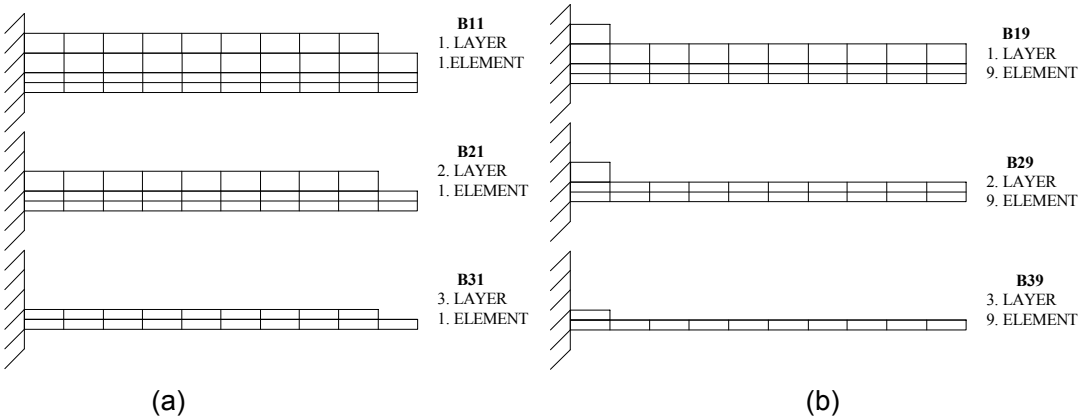

Figure 2: Beam models at the end of (a) 1st and (b) 9th step of 1st, 2nd and 3rd cuts.

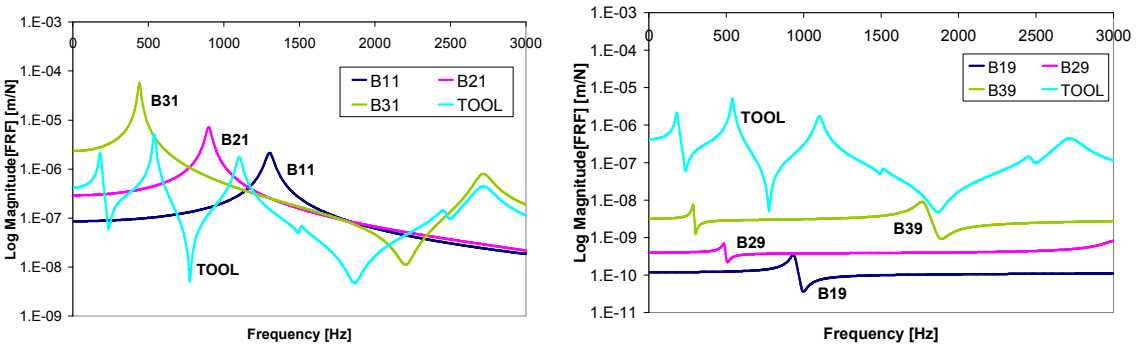

(a) (b)

Figure 3: FRFs of the workpiece and the tool at the end of (a) 1st and (b) 9th step of 1st, 2nd and 3rd cuts.

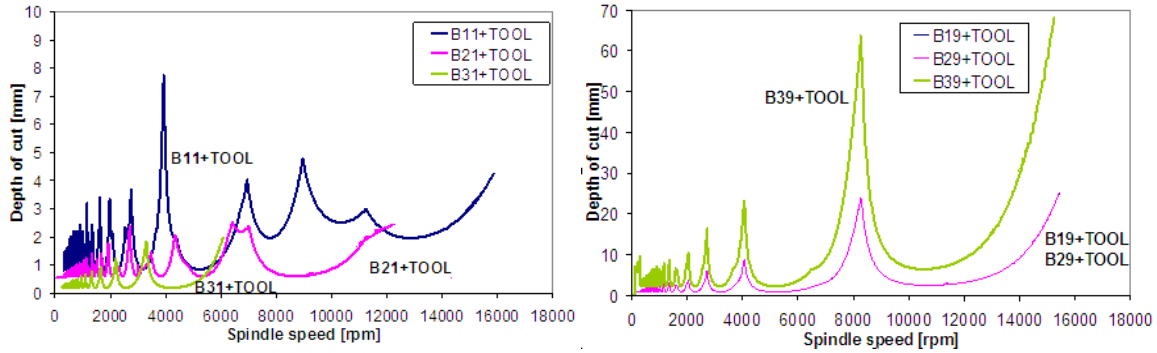

(a) (b)

Figure 4: Stability lobe diagram including the FRFs of the workpiece at the end of (a) first and (b) ninth step of 1st, 2nd and 3rd cuts.

As shown in Figure 4, the stability limits (both absolute and peak) becomes lower as the thickness of the workpiece is reduced as expected. The amount of change in the FRF peak amplitudes as a result of the mass removal can be different for different modes of the structure. Then, the stability lobes corresponding to different modes can move up or down, and left and right resulting in various forms of intersections among them. As a result, in addition to the reduced absolute and peak stability limits, some stability pockets may disappear as the workpiece becomes thinner. The spindle speeds corresponding to the peaks of the stability curve usually move to lower speeds with increasing flexibility of the workpiece.
As shown in Figure 4(b), the stability curves are the same for all cuts at this location except the finishing cut where the radial depth of cut is different than the previous two cuts. Note that since the stability diagrams of B19 and B29 are almost the same, they seem as one curve in the figure. It can be concluded that the variation of the workpiece dynamics does not affect the stability limits when the tool is much more flexible in which case the workpiece dynamics can be neglected.

4.2 Variation of Stable Spindle Speeds and Depth of Cuts

In this section, the effects of the part dynamics variation as a result of the mass removal are demonstrated in terms of stable depth of cuts and corresponding spindle speeds. The stability diagrams at different steps of machining are shown in Figure 5 where the variation of the stable depths and lobe locations due to mass removal can be seen. The variation in the maximum stable depth of cut and the corresponding spindle speeds for the 1st and 2nd lobes are given in Figure 6.

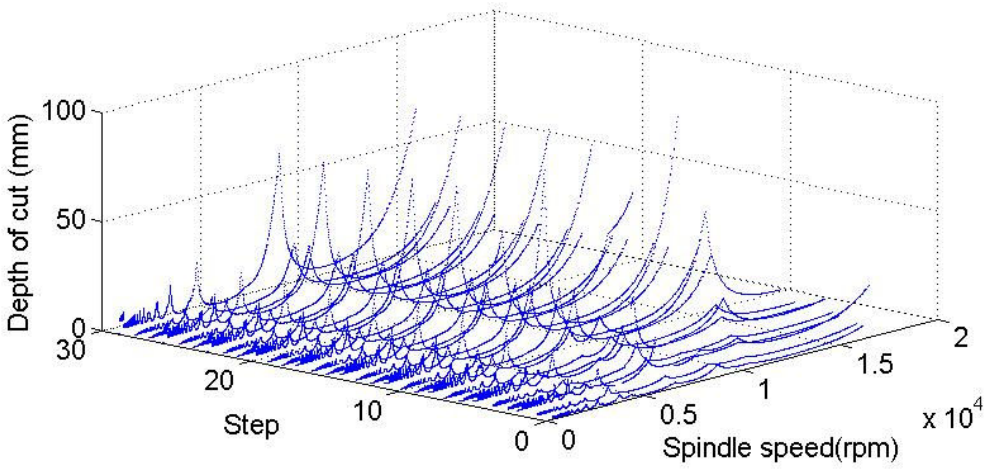

Figure 5: Stability diagrams at different steps of machining.

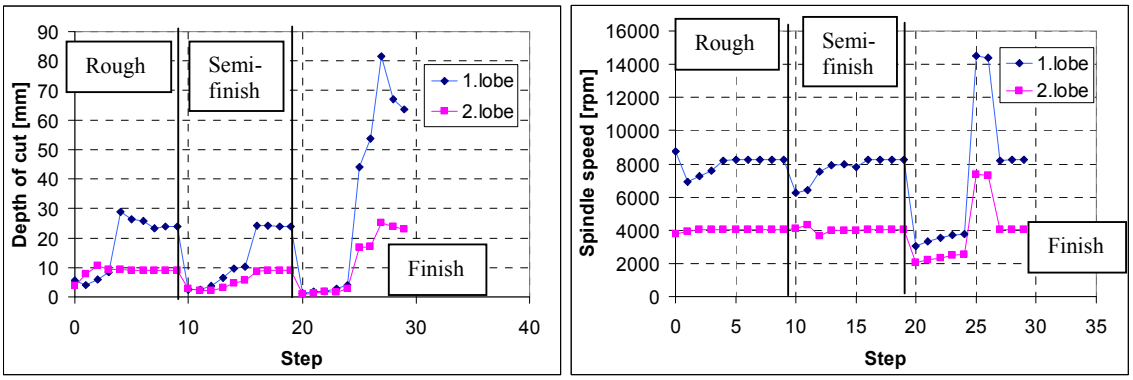

(a) (b)

Figure 6: Variation of (a) the stable depth of cuts and (b) the spindle speeds for the 1st and 2nd stability lobes during machining of the workpiece.

The variation patterns for the stable spindle speeds and depth of cuts can be explained by examining the FRF variations during machining as presented in the previous sections. For instance, in the roughing cycle from 1st step to 4th step, since the FRFs of the workpiece are higher than those of the tool, the workpiece dynamics become dominant. As the amplitudes of the workpiece's FRFs reduce from the free-end to the middle, the stable depth of cuts increase. After the 4th step, the FRFs of the tool become more flexible, and the variation in the stable depths and speeds nearly remain constant. The same trend can be observed in the semi-finishing cut as well. In the finishing cut, the workpiece becomes very flexible, and the increase in the stable depths continues until the 7th step.

The stable spindle speeds corresponding to stable depth of cuts nearly remain constant in the roughing and the semi-finishing cycles where only at the 1st and 2nd steps some decrease is observed. This decrease in the stable spindle speeds which corresponds to the machining at the free end is more significant in the finishing cycle since the workpiece becomes significantly flexible at these steps. In conclusion, the variations in chatter-free depth of cuts and spindle speeds are consistent with the variation in the workpiece dynamics, and the influence of the workpiece flexibility on the chatter stability can be observed easily when the workpiece is as flexible as the tool.

4.3 Effect of Radial Depth of Cut on the Stable Machining Time

In this section, the effect of the radial depth of cut on the stability is discussed through two alternative machining processes having different radial depths in the roughing, semi-finishing and finishing cycles. The same beam and tool-holder-spindle models presented before are used. The thickness of the workpiece is reduced from 15 mm to 3 mm by three main cuts as shown in Table 1.

Table 1: Radial depth of cut for every cycle of the first and second process alternatives

	Radial Depth of Cut	
	First Process	**Second Process**
Roughing	5 mm	7 mm
Semi-finishing	5 mm	4 mm
Finishing	2 mm	1 mm

The axial depth of cut is taken as 10 mm as an initial assumption so that the workpiece is machined in 10 steps per cut. The stable machining times calculated for the first process in the roughing, semi-finishing and finishing cuts, are compared with those for the second machining as shown in Table 2.

Table 2: Stable machining times for every cycle of the first and second process alternatives

	First Process			**Second Process**		
	Spindle speed(rpm)	**Depth of cut(mm)**	**Time (min)**	**Spindle speed(rpm)**	**Depth of cut(mm)**	**Time (min)**
Roughing cut	8940	3.32	0.29	9135	1.92	0.48
Semi-finishing cut	6413	1.29	1.52	5138	0.79	3.07
Finishing cut	3143	0.53	7.52	2465	1.03	4.97
		Total time(min)	9.33		**Total time(min)**	8.52

Since the radial depth of the cut in the roughing cycle of the second process (7 mm) is larger than that in the first one (5 mm), the stable axial depth of cut is lower for the second process. As a result, the roughing takes longer for the second process. The semi-finishing time is longer for the second process again due the difference in the flexibility of the workpiece in two processes (10 mm vs. 8 mm part thickness). Thus, the stable axial depth of cut is smaller in the second process due to higher workpiece flexibility resulting in longer machining time. In finishing, however, the second process with smaller radial depth of cut (1 mm) takes shorter time than the first process with radial depth of cut of 2 mm.

The machining times determined by using the second method described in section 3.3 are given in Tables 3 for both process alternatives. Note that for the second method the maximum possible stable axial depth is used for each pass of every cycle.

Table 3: Stable machining times for the first and second process alternatives using the second method in axial depth selection

	First Process	**Second Process**
	Total Time (min)	**Total Time (min)**
Roughing cut	0.15	0.19
Semifinishing cut	0.40	0.76
Finishing cut	1.63	1.49
Full machining time (min)	2.18	2.44

As it can be seen from the above table, the stable machining time is significantly reduced by using the second method compared to the first one (about 2 minutes vs. 9 minutes). This is

expected as the maximum possible stable depth of cut is used for each pass in the second method whereas in the first method is very conservative since the minimum stable depth must be used for the whole cycle. This fact, although obvious, is critical for production operations as the second method is commonly applied for tool path generation in almost all commercial CAM systems. Variable depth can be obtained, manually or semi-manually, increasing the programming time, however, due to the savings in the production times this would be well justified. Depending on the tool and part geometry, variable depth may not be used in the some finishing cases due to the surface quality requirements such as in the case of airfoil surfaces where the depth or the step size is determined based on the allowable scallop height. However, variable depth can be used in roughing and semi-finishing even for these cases.
The machining time trends observed with the first and the second process parameters before can also be seen in the second machining method. Thus, in addition to the use of variable axial depth of cut, the machining time can also be shortened by selecting the radial depth of cuts properly in the milling of a flexible part.

4.4 Effect of Different Cutting Strategies on the Stable Machining Time

Different strategies can be used in the machining of a part, and in this section the effect of cutting patterns on the stability is discussed. For instance, in the methods used in the previous sections, in a cutting cycle the workpiece's thickness was reduced by the same amount everywhere. This cutting pattern will be called as "layer removal". In another cutting strategy the workpiece's thickness can be reduced to its final thickness at the same location. For instance, in the first step the thickness of the free end of the workpiece can be reduced from 15 mm to 10 mm. At the second step, the thickness of the same location can be reduced from 10 mm to 5 mm, and at the third step this thickness can be reduced to 3 mm as shown in Figure 7. The same cutting pattern can be repeated along the part surface until the final thickness is obtained everywhere. This cutting pattern will be called as "step removal". Note that step removal can only be applied in practice if the same cutting tool is used in all cutting cycles, i.e. roughing, semi-finishing and finishing. Otherwise, tools must be changed very frequently resulting in long waiting times. The beam and tool-holder-spindle models used before are also used in this machining process.

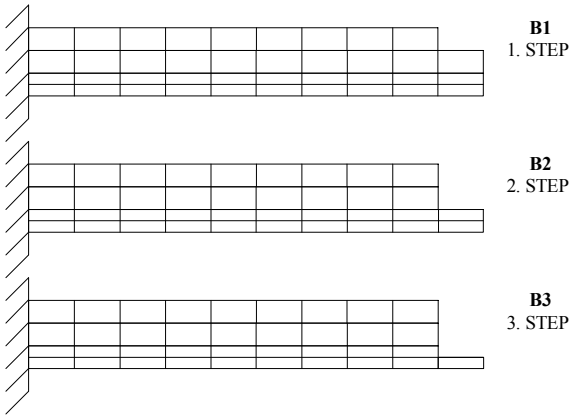

Figure 7: Beam models at the end of 1st, 2nd and 3rd steps in the "step removal" cutting.

First and second machining processes with different radial depth of cuts which are used in section 4.3 can be studied by using step removal machining pattern. Again the axial depth of cut is taken as 10 mm as an initial assumption.
In this section, the chatter-free machining time of the step removal process is calculated using the second method, i.e. using variable axial depth of cut. The stability diagrams at different machining steps can be seen in Figure 8, and used in the calculation of the stable machining times. The total machining times of two processes with the step removal pattern are given in Table 4.

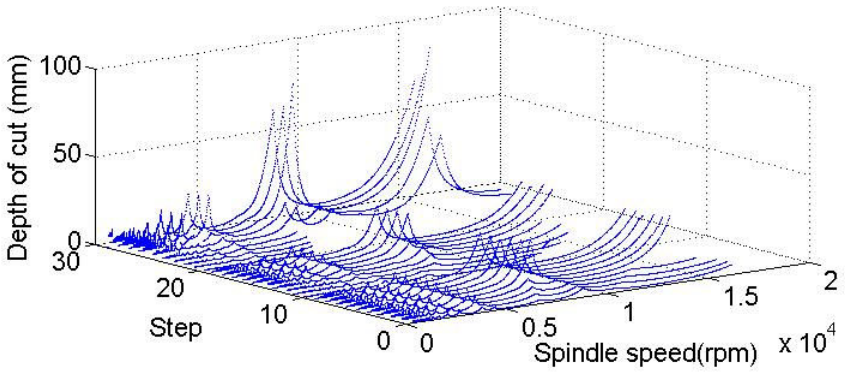

Figure 8: Stability diagrams at different machining steps for layer removal method.

Table 4: Stable machining times using the step removal process and the second method

	First Process	Second Process
	Total Time(min)	Total Time(min)
Step Removal	0.48	0.48

Full machining time of the step removal process is 0.48 minutes compared to 2.18 and 2.44 minutes in the layer removal process. The layer removal takes about 5 times longer than the step removal process, thus the stable cycle time can be shortened significantly using the step removal. The reason for this can be explained by examining the rigidity of the parts during machining with both methods. In the step removal method, the thickness of the part at the fixed end is kept at its maximum throughout the whole process, and thus the stiffness of the part is much higher compared to the layer removal. Similar cutting patterns can be developed by examining the workpiece geometry, cutting and boundary conditions, and the machining time can be minimized by using maximum stabile depths and an efficient cutting strategy.

5 CONCLUSIONS

In this study, the effect of workpiece dynamics on the prediction of the stability is studied in detail. The changing dynamics of the workpiece during the machining process was determined using the matrix inversion method for structural modification analysis where the FRFs were obtained by the FEA. The effects of the variation of the workpiece dynamics on the system FRFs and chatter stability were examined by using the analytical stability diagrams. It is observed that mainly two important parameters affect the FRFs of the workpiece. The first is the location where the FRFs of the workpiece are calculated (tool contact location). The case studies performed in this study showed that the FRFs of the workpiece at the free end take the highest value compared to the other locations. The second parameter is the change in the thickness of the machined workpiece. As the workpiece gets thinner during machining, the magnitudes of the FRFs of the workpiece become higher. Also, the modal frequencies become lower with the decreasing thickness resulting in variations of the stability lobe locations. The effects of the radial depth of cut and machining strategy on the stability diagrams were also investigated. It is observed that by using a cutting pattern which is selected by considering the geometry of the workpiece, the stability limits of the system can be increased and the machining time can be reduced significantly. The results presented here show the importance of the workpiece dynamics and its variation, and can be used in the selection of stable process parameters and high productivity machining strategies.

6 REFERENCES

[1] Taylor, F.W.,1907, On the Art of Cutting Metals, ASME Trans 28, 31-350.
[2] Tobias, S.A., Fishwick, W., 1958, The chatter of lathe tools under orthogonal cutting conditions, Transactions of ASME 80, 1079-1088.
[3] Tobias, S.A., 1965, Machine Tool Vibration, Blackie and Sons Ltd.

[4] Tlusty, J., Polacek, M., 1963, The stability of machine tools against self excited vibrations in machining, International Research in Production Engineering, ASME, 465-474.
[5] Merrit, H., 1965, Theory of self-excited machine tool chatter, Transactions of ASME Journal of Engineering for Industry 87, 447-454.
[6] Koenisberger, F., Tlusty, J., 1967, Machine Tool Structures – vol. I: Stability Against Chatter, Pergamon Press, Englewood Cliffs, NJ .
[7] Opitz, H., 1968, Chatter behavior of heavy machine tools. Quarterly Technical Report No. 2 AF61 (052)-916. Research and Technology Division, Wright-Patterson Air Force Base, OH.
[8] Opitz, H., Bernardi, F., 1970, Investigation and calculation of the chatter behavior of lathes and milling machines. Annals of the CIRP. 18: 335-343.
[9] Tlusty, J., Ismail, F., 1981, Basic nonlinearity in machining chatter, Annals of the CIRP 30, 21-25.
[10] Tlusty, J., 1986, Dynamics of high-speed milling, Transactions of ASME Journal of Engineering for Industry 108 (2), 59-67.
[11] Smith, S., Tlusty, J., 1993, Efficient simulation programs for chatter in milling, Annals of the CIRP 42 (1) 463-466.
[12] Sridhar, R., Hohn, R.E., Long, G.W., 1968, General formulation of the milling process equation, ASME Journal of Engineering for Industry. 317-324.
[13] Sridhar, R., Hohn, R.E., Long, G.W., 1968, A stability algorithm for the general milling process, ASME Journal of Engineering for Industry, 330-334.
[14] Minis, I., Yanushevsky, T., Tembo, R., Hocken, R., 1990, Analysis of linear and nonlinear chatter in milling, Annals of the CIRP 39, 459-462.
[15] Minis, I., Yanushevsky, T., 1993, A new theoretical approach for prediction of machine tool chatter in milling, ASME Journal of Engineering for Industry, 115, 1-8.
[16] Altintas, Y., Budak, E., 1995, Analytical prediction of stability lobes in milling, Annals of the CIRP 44, 357-362.
[17] Budak, E., Altintas, Y., 1998, Analytical prediction of chatter stability in milling – part I: general formulation; part II: application to common milling systems, Transactions of ASME, Journal of Dynamic Systems, Measurement, and Control, 120, 22-36.
[18] Altintas, Y., 2000, Manufacturing Automation, Cambridge University Press, Cambridge.
[19] Ertürk, A., Özgüven, H.N., Budak, E., 2006, Analytical modeling of spindle-tool dynamics on machine tools using Timoshenko beam model and receptance coupling for the prediction of tool point FRF, International Journal of Machine Tools and Manufacture, 46, 1901-1912.
[20] Budak, E., Ertürk, A., Özgüven, H.N., 2006, A modeling approach for analysis and improvement of spindle-holder-tool assembly dynamics, Annals of the CIRP 55, 369-372.
[21] Ertürk, A., Özgüven, H.N., Budak, E., 2007, Effect analysis of bearing and interface dynamics on tool point FRF for chatter stability in machine tools by using a new analytical model for spindle-tool assemblies, Int. Journal of Machine Tools and Manufacture, 47(1), 23-32.
[22] Ertürk, A., Budak, E., Özgüven, H.N., 2007, Selection of design and operational parameters in spindle-holder-tool assemblies for maximum chatter stability by using a new analytical model, International Journal of Machine Tools and Manufacture, 47, 1401-1409.
[23] Özgüven, H.N., 1984, Determination of receptances of locally damped structures, Proceedings of the Second International Conference on Recent Advances in Structural Dynamics, Vol. 2, 887-892.
[24] Özgüven, H.N., 1987, A new method for harmonic response of non-proportionally damped structures using undamped modal data, Journal of Sound and Vibration, 117, 313-328.
[25] Özgüven, H.N., 1990, Structural modifications using frequency response functions, Mechanical Systems and Signal Processing, Vol. 4, n.1, 53-63.
[26] Ozlu, E., Budak, E., 2007, Comparison of one dimensional and multi dimensional models in stability analysis of turning operations, International Journal of Machine Tools and Manufacture, Vol. 47, pp. 1875-1883.
[27] Budak, E., Altintas, Y., Armarego, E.J.A., 1996, Prediction of Milling Force Coefficients From Orthogonal Cutting Data, Trans. ASME Journal of Manufacturing Science and Engineering, 118, 216-224.
[28] Budak, E., 2006, Analytical models for high performance milling. Part II: Process dynamics and stability, International Journal of Machine Tools & Manufacture 46, 1489–1499.
[29] Budak, E., 2006, Analytical models for high performance milling. Part II: Process dynamics and stability, International Journal of Machine Tools & Manufacture 46, 1489–1499.